

Effect of pressure on the structural phase transition and superconductivity in $(\text{Ba}_{1-x}\text{K}_x)\text{Fe}_2\text{As}_2$ ($x=0$ and 0.45) and SrFe_2As_2 single crystals

M. S. Torikachvili

Department of Physics, San Diego State University, San Diego, California 92182-1233, USA

S. L. Bud'ko, N. Ni, and P. C. Canfield

Ames Laboratory, US DOE and Department of Physics and Astronomy, Iowa State University, Ames, Iowa 50011, USA

(Received 7 July 2008; published 29 September 2008)

The effects of pressure up to ~ 20 kbar on the structural phase transition of SrFe_2As_2 and lightly Sn-doped BaFe_2As_2 as well as on the superconducting transition temperature and upper critical field of $(\text{Ba}_{0.55}\text{K}_{0.45})\text{Fe}_2\text{As}_2$ single crystals have been studied. All the transition temperatures decrease with pressure in an almost linear fashion. Under pressure, the upper critical-field curve $H_{c2}(T)$ for $(\text{Ba}_{0.55}\text{K}_{0.45})\text{Fe}_2\text{As}_2$ shifts down in temperature to follow the zero-field T_c with very little change in slope. Composite P - T phase diagrams for three parent compounds $A\text{Fe}_2\text{As}_2$ ($A=\text{Ba},\text{Sr},\text{Ca}$) are constructed and appear to be remarkably similar: (i) having a structural (antiferromagnetic) phase-transition line with a negative slope and (ii) showing signs of the emerging superconducting state at intermediate pressures.

DOI: [10.1103/PhysRevB.78.104527](https://doi.org/10.1103/PhysRevB.78.104527)

PACS number(s): 61.50.Ks, 74.62.Fj, 74.70.Dd

I. INTRODUCTION

The recent reports of the discovery of elevated temperature superconductivity in $\text{LaFeAs}(\text{O}_{1-x}\text{F}_x)$ (Ref. 1) followed by an almost twofold increase in the superconducting transition temperature by application of pressure² or by substitution of heavier rare earths³ have brought a lot of attention to materials with structures containing Fe-As layers. Within a few months, superconductivity below $T_c=38$ K was discovered in the structurally related, nonoxide material, K-doped BaFe_2As_2 (Ref. 4), and single crystals of the parent, non-superconducting compound BaFe_2As_2 , as well as superconducting $(\text{Ba}_{0.55}\text{K}_{0.45})\text{Fe}_2\text{As}_2$ were synthesized.^{5,6} Although the parent compound appears to be sensitive to small, $\sim 1\%$, of Sn doping⁵⁻⁷ (light doping of Sn is an unintended consequence of the crystal-growth process) a small amount of Sn do not seem to be detrimental for superconductivity in the K-doped compound.^{4,5} Single crystals of pure and K-doped SrFe_2As_2 have also been synthesized.^{8,9} SrFe_2As_2 bears similarity to BaFe_2As_2 in having structural (antiferromagnetic) phase transition at ~ 200 K and exhibiting superconductivity at elevated temperatures upon K doping.

Pressure was shown to have a remarkable effect on low-temperature behavior of CaFe_2As_2 .¹⁰ The structural (antiferromagnetic) transition is rapidly suppressed under pressure and is observed up to $P\approx 3.5$ kbar; at ~ 5.5 kbar a new transition, marked by a decrease in resistivity, is detected at ~ 104 K, increasing to above 300 K by 19 kbar. At low temperatures, pressure-induced superconductivity ($T_c\leq 12$ K is observed between approximately 2.3 and 8.6 kbar). Similarly, superconducting domes were reported for BaFe_2As_2 and SrFe_2As_2 under pressure¹¹ but with no data on the effects of pressure on the structural/antiferromagnetic transition. In order to compare the P - T phase diagrams of BaFe_2As_2 and SrFe_2As_2 with the one for CaFe_2As_2 ,¹⁰ and to probe the assumed similarities between doping and pressure in these compounds, in this work we study the effect of hydrostatic pressure on parent, lightly Sn-doped BaFe_2As_2 ,

superconducting $(\text{Ba}_{0.55}\text{K}_{0.45})\text{Fe}_2\text{As}_2$, as well as parent SrFe_2As_2 single crystals.

II. EXPERIMENTAL DETAILS

Single crystals of BaFe_2As_2 , $(\text{Ba}_{0.55}\text{K}_{0.45})\text{Fe}_2\text{As}_2$, and SrFe_2As_2 were grown out of a Sn flux using conventional high-temperature solution growth techniques.¹² The details of the growth as well as thermodynamic and transport properties of these crystals are described in Refs. 5 and 8. At ambient pressure the structural phase transition in BaFe_2As_2 is marked by a rapid increase in in-plane resistivity, whereas in SrFe_2As_2 in-plane resistivity abruptly decreases below such transition. The pressure dependencies of the structural phase-transition temperature T_0 , the superconducting phase-transition temperature T_c , and the upper critical-field H_{c2} were determined from the temperature-dependent in-plane resistance. Pressure was generated in a Teflon cup filled with either a 60:40 mixture of n pentane and light mineral oil or Fluorinert FC-75 inserted in a 22-mm-outer-diameter, non-magnetic, piston-cylinder-type, Be-Cu pressure cell with a core made of NiCrAl (40 KhNYu-VI) alloy. The pressure at room temperature was monitored by a manganin, resistive pressure gauge. At low temperatures the pressure value was determined from the superconducting transition temperature of pure lead.¹³ Low-temperature pressure values will be used throughout most of the text as the pressure remains almost constant in similar geometry cells on cooling below ~ 100 K.¹⁴ The data for the pressure dependent room-temperature resistance and structural (antiferromagnetic) transition in SrFe_2As_2 use either room-temperature values of pressure or an interpolation of pressures for intermediate temperatures. The temperature and magnetic-field environment for the pressure cell was provided by a Quantum Design Physical Property Measurement System (PPMS-9) instrument. An additional Cernox sensor, attached to the body of the cell, served to determine the temperature of the sample for these measurements. The cooling rate was below 0.5

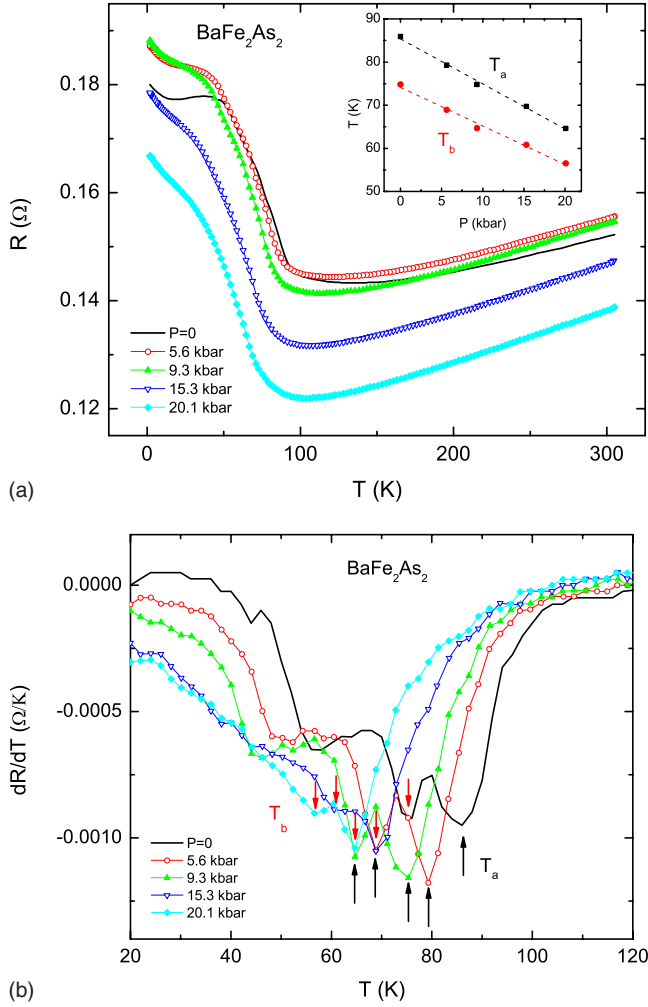


FIG. 1. (Color online) (a) Pressure dependence of in-plane resistance of BaFe_2As_2 . [For BaFe_2As_2 sample $\rho_{300\text{ K}}(P=0) \approx 1\text{ m}\Omega\text{ cm}$.] Inset: pressure dependent transition temperatures, determined as shown in panel (b), the lines are from linear fits. (b) Derivatives dR/dT at different pressures in the transition region. Arrows show two definitions of the transition temperature (Ref. 5).

K/min, the temperature lag between the Cernox on the body of the cell, and the system thermometer was $<0.5\text{ K}$ at high temperatures and 0.1 K or less, below $\sim 70\text{ K}$.

III. RESULTS

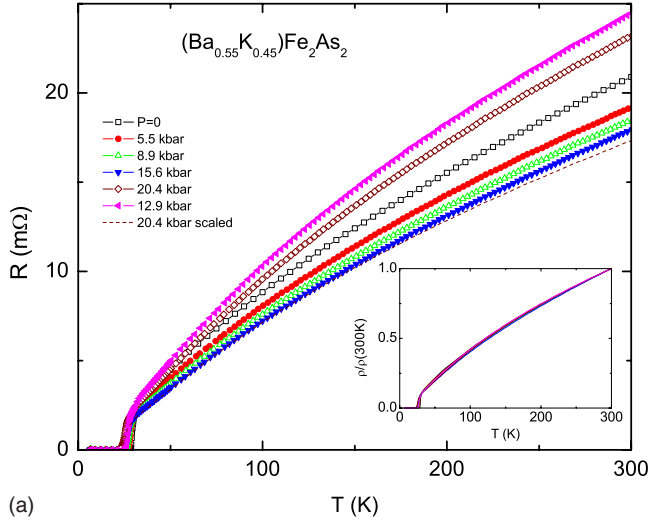
Figure 1(a) shows the temperature-dependent resistance of BaFe_2As_2 at different pressures. Above $\sim 10\text{ kbar}$ the $\rho(T)$ curves shift down with pressure, qualitatively similar to high-temperature (above the phase transitions) resistance of CaFe_2As_2 .¹⁰ Although the feature in resistivity corresponding to the structural phase transition is somewhat broad, its pressure dependence can be monitored by following the pressure evolution of the minima in the derivative dR/dT [Fig. 1(b)]. It is worth noting that although the resistive anomaly appears to be associated with a single transition (a conclusion supported by ambient pressure data⁵), at least two minima can be seen in dR/dT [marked with up- (T_a) and down- (T_b) ar-

rows in Fig. 1(b)]. Both minima shift to lower temperatures [inset in Fig. 1(a)] under pressure with similar pressure derivatives $dT_a/dP = -1.04 \pm 0.04\text{ K/kbar}$, $dT_b/dP = -0.89 \pm 0.05\text{ K/kbar}$, giving further support to the assumption that this anomaly is associated with a single transition and that the fine structure in dR/dT is an artifact. Using a linear extrapolation of these data, the structural phase transition can be expected to be suppressed by $\sim 80\text{ kbar}$. This is most likely an upper limit, given the possibility of superlinear suppression at higher pressures.

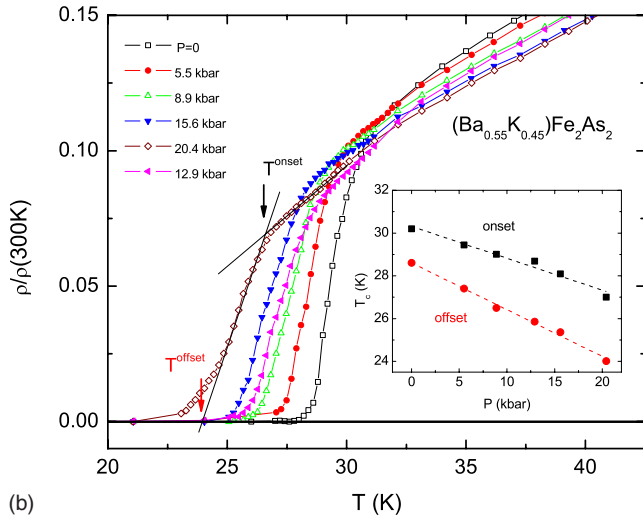
For superconducting $(\text{Ba}_{0.55}\text{K}_{0.45})\text{Fe}_2\text{As}_2$, the normal-state resistivity decreases under pressure [again, similarly to CaFe_2As_2 (Ref. 10)] through $\sim 15\text{ kbar}$ as shown in Fig. 2(a). The normal-state resistance values for the next pressure, 20.4 kbar, jump upwards, however this jump seems to be extrinsic since the normal state $R(T)$ retains a positive offset when we back off the pressure to 12.9 kbar. It seems reasonable to assume that this resistance jump after the fourth pressure run was caused by some change in the geometric factor of the sample, such as development of a small crack. Indeed, the normalized resistivity $\rho(T)/\rho(300\text{ K})$ does not change significantly with pressure. Based on this, it is worth noting that [Fig. 2(a), inset] the 20.4 kbar run yields data consistent with the first four pressure runs' normal-state resistance values if they are scaled with the last, 12.9 kbar, curve, as shown in Fig. 2(a). It should be emphasized that this jump in the normal-state resistance has no bearing on the superconducting transition temperature behavior under pressure.

The superconducting transition temperature decreases under pressure with some (reversible) broadening of the resistive transition [Fig. 2(b)]. For different criteria in the determination of T_c , the pressure derivatives are $dT_c^{\text{onset}}/dP = -0.15 \pm 0.01\text{ K/kbar}$ and $dT_c^{\text{offset}}/dP = -0.21 \pm 0.01\text{ K/kbar}$ [Fig. 2(b)]. The upper critical field in $(\text{Ba}_{0.55}\text{K}_{0.45})\text{Fe}_2\text{As}_2$ is expected to be extremely high, on the order of 1,000 kOe.^{5,15,16} Our measurements, up to 90 kOe, can probe only a small section of the $H_{c2}(T)$ curve, close to zero-field T_c . The $P=0$ $H_{c2}(T)$ data are similar to that in Ref. 5. Under pressure, the $H_{c2}(T)$ appear to shift (Fig. 3), following the shift of T_{c0} without changes in the slope or curvature.

The temperature-dependent resistance of SrFe_2As_2 at different pressures is shown in Fig. 4. Applied pressure noticeably lowers the high-temperature (tetragonal phase) resistance, as has been the case for CaFe_2As_2 , BaFe_2As_2 , and $(\text{Ba}_{0.55}\text{K}_{0.45})\text{Fe}_2\text{As}_2$. The sharp resistance anomaly associated with the tetragonal to orthorhombic, structural phase-transition temperature⁸ is suppressed under pressure. These results are similar to those presented in Ref. 17 on polycrystalline and Bridgeman-grown single crystalline SrFe_2As_2 . The low-temperature part of the $R(T)$ curves has an additional feature (Fig. 4, lower right inset). This feature T^* is marked by a sharp—but continuous—decrease in resistance, is seen in $P=0$ data with some ambiguity, but is unambiguously present at all elevated pressures. It should be noted, though, that this transition does not give any clear indication of producing zero resistance. This feature is only slightly field dependent; for $P=18.9\text{ kbar}$ data T^* shifts down by $\approx 4\text{ K}$ ($<15\%$) at 90 kOe magnetic field ($H \perp c$). Figure 5 summarizes the pressure dependencies of the two transition temperatures for SrFe_2As_2 . The decrease in the structural



(a)



(b)

FIG. 2. (Color online) (a) Temperature-dependent in-plane resistance of $(\text{Ba}_{0.55}\text{K}_{0.45})\text{Fe}_2\text{As}_2$ under pressure (pressure values in the legend are in the order of runs). [For $(\text{Ba}_{0.55}\text{K}_{0.45})\text{Fe}_2\text{As}_2$ sample $\rho_{300\text{ K}}(P=0) \approx 0.9\text{ m}\Omega\text{ cm}$.] Dashed line—20.4 kbar data scaled in a way that brings the last, 12.9 kbar, data between 8.9 and 15.6 kbar runs. Inset: normalized temperature-dependent resistivity as a function of pressure. (b) Resistive superconducting transition in $(\text{Ba}_{0.55}\text{K}_{0.45})\text{Fe}_2\text{As}_2$ (pressure values in the legend are in the order of runs). Inset: superconducting transition temperatures (defined as onset and offset of resistive transition) as a function of pressure. The lines are from linear fits (Ref. 5).

(antiferromagnetic) transition temperature under pressure is somewhat nonlinear as well, by 20 kbar the transition temperature is $\sim 86\%$ of its $P=0$ value, and a gross extrapolation of its pressure dependence suggests that the structural transition may be suppressed by ~ 80 kbar. T^* depends on pressure nonmonotonically and apparently just starts to increase near the limit of the present measurements.

IV. DISCUSSION AND SUMMARY

Of three parent AFe_2As_2 ($\text{A}=\text{Ba}$, Sr , and Ca) compounds, the pressure-temperature phase diagram of CaFe_2As_2 is at

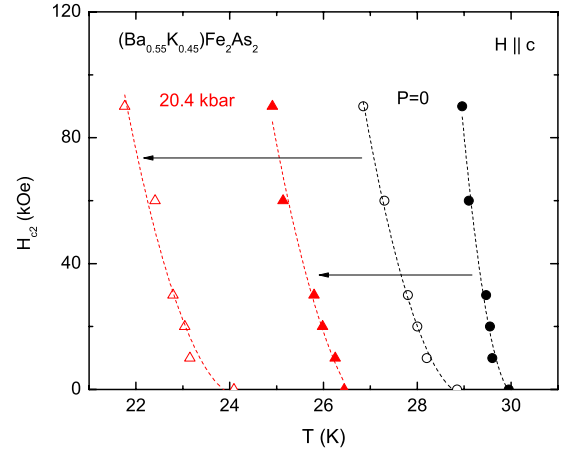


FIG. 3. (Color online) Upper critical fields $H_{c2}(T)$ measured up to 90 kOe at zero and maximum pressures as defined from onset (filled symbols) and offset (open symbols) of resistive transitions. The lines are guides to the eye.

this point studied in the greatest detail. At room temperature and ambient pressure the material has a tetragonal structure and is not magnetically ordered.¹⁸ On cooling, at ambient pressure, a structural, tetragonal to orthorhombic, first order, phase transition, coincident with a transition to long-range antiferromagnetically ordered phase occurs at ~ 170 K.^{18,19} On application of very moderate (~ 3 kbar) pressure, superconductivity below ~ 12 K, as evidenced by zero resistivity and enhanced diamagnetic signal,^{10,20} is observed. On further increase in pressure, the superconducting transition tempera-

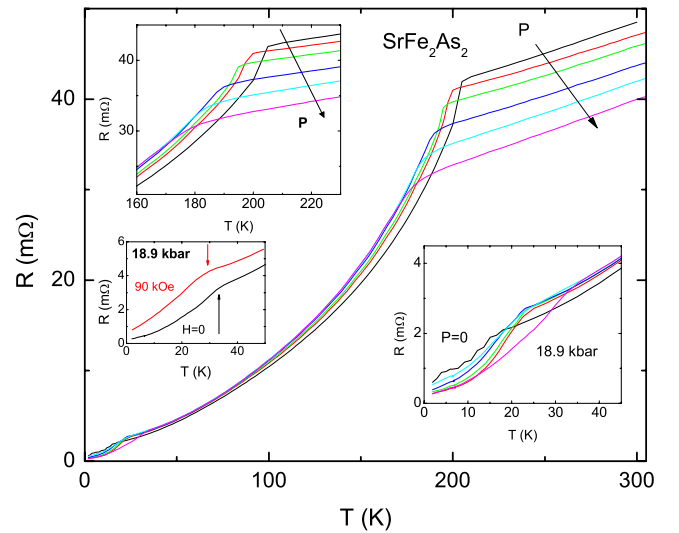


FIG. 4. (Color online) Temperature-dependent in-plane resistance of SrFe_2As_2 measured at $P=0, 3.1, 6.4, 12.1, 15.7,$ and 18.9 kbar (pressure values at low temperatures). Arrow indicates the direction of the pressure increase. Upper left inset: enlarged region of the $R(T)$ curves near the structural (antiferromagnetic) phase transition. Arrow indicates the direction of the pressure increase. Lower right inset: enlarged low-temperature part of the $R(T)$ curves in the region of the T^* (see text). Lower left inset: low-temperature part of the $R(T)$ curves taken at $P=18.9$ kbar for $H=0$ and 90 kOe. Vertical arrows mark T^* .

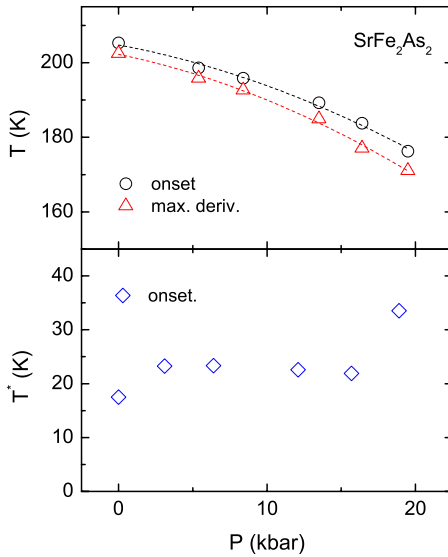


FIG. 5. (Color online) Pressure dependence of the structural (antiferromagnetic) phase transition (top panel) and T^* low-temperature anomaly (bottom panel). Pressure values interpolation consistent with Ref. 14 were used for the top panel and low-temperature values of pressure for $T^*(P)$. Two criteria, onset and maximum of the dR/dT derivatives, were used for the structural (antiferromagnetic) transition.

ture slightly increases, then decreases, and vanishes above ~ 9 kbar. Starting from $P > 5$ kbar, a new, high-temperature, highly hysteretic, feature in resistivity with its critical temperature rapidly rising under pressure is observed.¹⁰ Recent neutron-diffraction studies under pressure²¹ revealed that this latter transition is from the high-temperature tetragonal phase to a low-temperature “collapsed” tetragonal phase with a dramatically smaller unit-cell volume and a loss of the lower pressure magnetic order. In the same study a low-temperature, almost vertical in P - T coordinates, phase boundary between the orthorhombic antiferromagnetic and collapsed tetragonal phases was suggested. A composite P - T phase diagram based on Refs. 10, 18, 19, and 21 is shown in Fig. 6(a). Our data on BaFe_2As_2 and SrFe_2As_2 can be used to create similar phase diagrams and for critical comparison.

Following the discovery of superconductivity under pressure in CeFe_2As_2 ,¹⁰ pressure-induced superconductivity above ~ 25 kbar was reported in BaFe_2As_2 and SrFe_2As_2 based on magnetic-susceptibility measurements.¹¹ Figure 6(b) presents a composite P - T phase diagram for BaFe_2As_2 that combines results of Ref. 11 and the present work (the crystals were grown in similar way in both cases). On a schematic level, this phase diagram is very similar to the one for CeFe_2As_2 [Fig. 6(a)]. At this time we are unaware of structural or electrical transport data for pressures above ~ 20 kbar, but such data, when available, will (i) shed light on how well this similarity between the P - T phase diagrams of CaFe_2As_2 and BaFe_2As_2 persists to higher pressures and (ii) reveal how clearly the superconductivity inferred by Ref. 11 manifests itself in resistivity data.

So as to compare the effects of pressure to chemical substitution, the $T_c(P^*)$ data for $(\text{Ba}_{0.55}\text{K}_{0.45})\text{Fe}_2\text{As}_2$ are added to the P - T phase diagram [Fig. 6(b)]. These data are plotted as

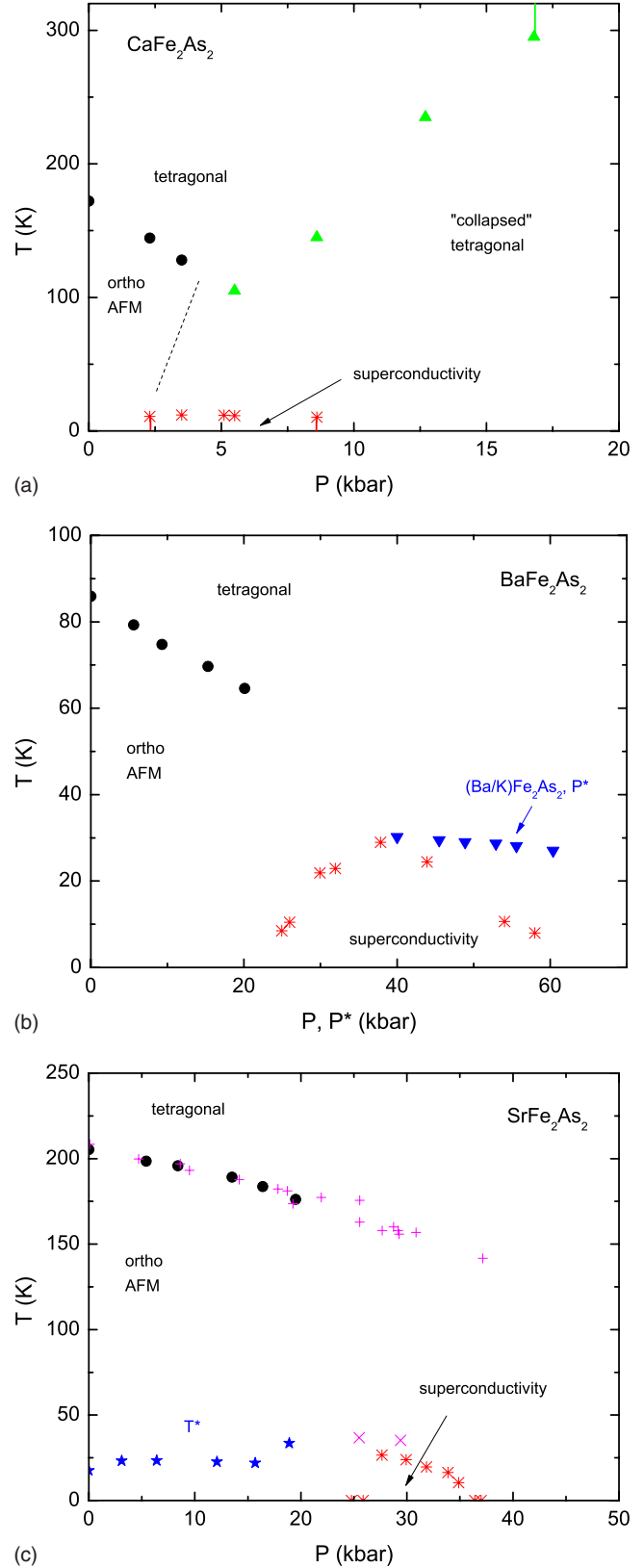


FIG. 6. (Color online) Schematic P - T phase diagrams for (a) CaFe_2As_2 , (b) BaFe_2As_2 , and (c) SrFe_2As_2 . Data in panel (a) are from Ref. 10. Panel (b) combines data from this work (\bullet), Ref. 11 ($*$), and shifted by 40 kbar data for $(\text{Ba}_{0.55}\text{K}_{0.45})\text{Fe}_2\text{As}_2$ (\star) from this work. Panel (c) presents data from this work (\bullet , \star), Ref. 11 ($*$), and Ref. 17 ($+$, \times).

a function of $P^* = P + 40$ kbar, shifted along the x axis so that the ambient pressure T_c for $(\text{Ba}_{0.55}\text{K}_{0.45})\text{Fe}_2\text{As}_2$ is close to the T_c value for pure BaFe_2As_2 under pressure on the side of the superconducting dome that has the same sign of dT_c/dP . This comparison plot shows that the T_c of the pure sample is much more sensitive to pressure than that of the doped sample. This suggests that pressure and doping are not strictly equivalent, and a parameter more complex than pressure is needed if one attempts to a scaling of superconducting transition temperatures in pure and doped BaFe_2As_2 .

In a similar manner, the results of the current work and the data from Refs. 11 and 17 for SrFe_2As_2 are summarized in the phase diagram shown in Fig. 6(c). The structural (antiferromagnetic) phase-transition temperature decreases with pressure in agreement with the literature data.¹⁷ On the other hand, the low-temperature part of the P - T phase diagram for this material appears to be more complex or subtle than those for the two other parent compounds in the AFe_2As_2 ($A = \text{Ba}, \text{Sr}, \text{Ca}$) family. Several points are worth noting. (i) The pressure-induced superconductivity inferred for this material¹¹ based on the observation of jump magnetic susceptibility is (shown as red asterisks) appeared to “turn on” at lower pressures in an abrupt manner. (ii) The low-temperature resistance feature at T^* , a clear loss of resistivity, found in this work (and shown as blue stars) is virtually identical to that observed in Ref. 17 for two pressures near 25 and 30 kbar (shown as magenta crosses). (iii) Both of these features are broad, and, unlike the case of CaFe_2As_2 ,¹⁰ the $R=0$ state was never observed. (iv) This T^* feature appears to be robust with respect to three different techniques of the samples preparation. (v) Placing the data from this work and from Refs. 11 and 17 on the same P - T diagram gives [Fig. 6(c)] rise to a domelike feature that extends down to as low as $P=0$ or at least $P=3.1$ kbar.

These data bring up the question whether the low-temperature T^* feature observed in SrFe_2As_2 under pressure is superconductivity, and if it is, whether the superconductivity is bulk. It is clear that further detailed, thermodynamic and transport measurements are needed to address the nature of the T^* feature and to confirm or refute the existence of a superconducting dome (bulk or otherwise) in SrFe_2As_2 . Given our data though, this study can be done at pressures as low as 3 or 6 kbar, rather than 20 kbar, allowing many more techniques and methods of generating pressure as possibilities. By analogy, a similar concern exists for BaFe_2As_2 as well. It is also worth noting that in CaFe_2As_2 there are low- and high-pressure features (even at $P=0$)^{10,18} that are similar to the low-temperature sharp resistance decrease at T^* seen at all pressures in SrFe_2As_2 . The primary difference in CaFe_2As_2 is that a full superconducting transition ($R=0$) was found for intermediate pressures.

To summarize, tetragonal to orthorhombic, structural (antiferromagnetic) phase transition is suppressed by pressure both in lightly Sn-doped BaFe_2As_2 and in SrFe_2As_2 with similar initial pressure derivatives $dT_s/dP \approx -1$ K/kbar that is approximately two times faster than in nonsuperconducting $\text{SmFeAs}(\text{O}_{0.95}\text{F}_{0.05})$ (Ref. 22) and an order of magnitude slower than in CaFe_2As_2 .¹⁰ A moderate pressure of ~ 80 kbar, or less, is expected to suppress the structural phase transitions completely in both materials.

For superconducting $\text{RFeAs}(\text{O}_{1-x}\text{F}_x)$ a variety of pressure dependencies have been reported: initial increase in T_c , followed by a maximum and almost decrease with pressure was reported for $\text{LaFeAs}(\text{O}_{0.89}\text{F}_{0.11})$,^{2,23} nonlinear T_c increase [$\text{LaFeAs}(\text{O}_{0.95}\text{F}_{0.05})$ (Ref. 2) and $\text{SmFeAs}(\text{O}_{0.87}\text{F}_{0.13})$ (Ref. 22)] or decrease [$\text{CeFeAs}(\text{O}_{0.88}\text{F}_{0.12})$ (Ref. 23)], as well as close-to-linear pressure dependencies of different signs and values [$\text{RFeAs}(\text{O}_{1-x}\text{F}_x)$ (Refs. 22 and 24)]. The negative, rather large, pressure derivative of T_c observed in $(\text{Ba}_{0.55}\text{K}_{0.45})\text{Fe}_2\text{As}_2$ is well within the range of the available data for oxygen-containing $\text{RFeAs}(\text{O}_{1-x}\text{F}_x)$. If compared with the literature data for pure BaFe_2As_2 (Ref. 11) it appears to be no simple, universal chemical/physical pressure scaling for pure and doped BaFe_2As_2 .

Composite P - T phase diagrams for three parent compounds, AFe_2As_2 ($A = \text{Ba}, \text{Sr}, \text{and Ca}$), appear to be remarkably similar in having structural (antiferromagnetic) phase-transition line with a negative slope and in either having clear or possible emergence of a superconducting state.

The results above suggest several extensions: (i) extension of electrical transport and x-ray/neutron-scattering measurements to 50–100 kbar range in search for a tetragonal to “collapsed” tetragonal structural phase-transition line in AFe_2As_2 ($A = \text{Ba}$ and Sr); (ii) low temperature, thermodynamic, and transport measurements in SrFe_2As_2 under pressure to understand the nature of the T^* anomaly and to confirm or refute the existence of pressure-induced superconductivity in this material; (iii) detailed study of pressure dependencies in K-doped materials with several values of K concentrations, if these samples can be reproducibly grown in single-crystal form; and (iv) high-field studies in $H_{c2}(T)$ under pressure.

ACKNOWLEDGMENTS

Work at the Ames Laboratory was supported by the U.S. Department of Energy-Basic Energy Sciences under Contract No. DE-AC02-07CH11358. M.S.T. gratefully acknowledges support from the National Science Foundation under Contracts No. DMR-0306165 and No. DMR-0805335. S.L.B. thanks Starik Kozlodoyev for relevant insights.

¹Y. Kamihara, T. Watanabe, M. Hirano, and H. Hosono, *J. Am. Chem. Soc.* **130**, 3296 (2008).

²H. Takahashi, K. Igawa, K. Arii, Y. Kamihara, M. Hirano, and H. Hosono, *Nature (London)* **453**, 376 (2008).

³X. H. Chen, T. Wu, G. Wu, R. H. Liu, H. Chen, and D. F. Fang, *Nature (London)* **453**, 761 (2008).

⁴M. Rotter, M. Tegel, and D. Johrendt, *Phys. Rev. Lett.* **101**, 107006 (2008).

- ⁵N. Ni, S. L. Bud'ko, A. Kreyssig, S. Nandi, G. E. Rustan, A. I. Goldman, S. Gupta, J. D. Corbett, A. Kracher, and P. C. Canfield, *Phys. Rev. B* **78**, 014507 (2008).
- ⁶X. F. Wang, T. Wu, G. Wu, H. Chen, Y. L. Xie, J. J. Ying, Y. J. Yan, R. H. Liu, and X. H. Chen, arXiv:0806.2452 (unpublished).
- ⁷M. Rotter, M. Tegel, D. Johrendt, I. Schellenberg, W. Hermes, and R. Pöttgen, *Phys. Rev. B* **78**, 020503(R) (2008).
- ⁸J.-Q. Yan, A. Kreyssig, S. Nandi, N. Ni, S. L. Bud'ko, A. Kracher, R. J. McQueeney, R. W. McCallum, T. A. Lograsso, A. I. Goldman, and P. C. Canfield, *Phys. Rev. B* **78**, 024516 (2008).
- ⁹G. F. Chen, Z. Li, J. Dong, G. Li, W. Z. Hu, X. D. Zhang, X. H. Song, P. Zheng, N. L. Wang, and J. L. Luo, arXiv:0806.2648 (unpublished).
- ¹⁰Milton S. Torikachvili, Sergey L. Bud'ko, Ni Ni, and Paul C. Canfield, *Phys. Rev. Lett.* **101**, 057006 (2008).
- ¹¹Patricia L. Alireza, Jack Gillett, Y. T. Chris Ko, Suchitra E. Sebastian, and Gilbert G. Lonzarich, arXiv:0807.1896, *J. Phys.: Condens. Matter* (to be published).
- ¹²P. C. Canfield and Z. Fisk, *Philos. Mag. B* **65**, 1117 (1992).
- ¹³A. Eiling and J. S. Schilling, *J. Phys. F: Met. Phys.* **11**, 623 (1981).
- ¹⁴J. D. Thompson, *Rev. Sci. Instrum.* **55**, 231 (1984).
- ¹⁵M. Altarawneh, K. Collar, C. H. Mielke, N. Ni, S. L. Bud'ko, and P. C. Canfield, arXiv:0807.4488 (unpublished).
- ¹⁶H. Q. Yuan, J. Singleton, F. F. Balakirev, G. F. Chen, J. L. Luo, and N. L. Wang, arXiv:0807.3137 (unpublished).
- ¹⁷M. Kumar, M. Nicklas, A. Jesche, N. Caroca-Canales, M. Schmitt, M. Hanfland, D. Kasinathan, U. Schwarz, H. Rosner, and C. Geibel, arXiv:0807.4283 (unpublished).
- ¹⁸N. Ni, S. Nandi, A. Kreyssig, A. I. Goldman, E. D. Mun, S. L. Bud'ko, and P. C. Canfield, *Phys. Rev. B* **78**, 014523 (2008).
- ¹⁹A. I. Goldman, D. N. Argyriou, B. Ouladdiaf, T. Chatterji, A. Kreyssig, S. Nandi, N. Ni, S. L. Bud'ko, P. C. Canfield, and R. J. McQueeney, *Phys. Rev. B* **78**, 100506(R) (2008).
- ²⁰M. S. Torikachvili, S. L. Bud'ko, N. Ni, and P. C. Canfield (unpublished).
- ²¹A. Kreyssig, M. A. Green, Y. Lee, G. D. Samolyuk, P. Zajdel, J. W. Lynn, S. L. Bud'ko, M. S. Torikachvili, N. Ni, S. Nandi, J. Leão, S. J. Poulton, D. N. Argyriou, B. N. Harmon, P. C. Canfield, R. J. McQueeney, and A. I. Goldman, arXiv:0807.3032 (unpublished).
- ²²B. Lorenz, K. Sasmal, R. P. Chaudhury, X. H. Chen, R. H. Liu, T. Wu, and C. W. Chu, *Phys. Rev. B* **78**, 012505 (2008).
- ²³D. A. Zocco, J. J. Hamlin, R. E. Baumbach, M. B. Maple, M. A. McGuire, A. S. Sefat, B. C. Sales, R. Jin, D. Mandrus, J. B. Jeffries, S. T. Weir, and Y. K. Vohra, *Physica C* **468**, 2229 (2008).
- ²⁴Y. Takabayashi, M. T. McDonald, D. Papanikolaou, S. Margadonna, G. Wu, R. H. Liu, X. H. Chen, and K. Prassides, *J. Am. Chem. Soc.* **130**, 9242 (2008).